

Article

Spiridonovite, $(\text{Cu}_{1-x}\text{Ag}_x)_2\text{Te}$ ($x \approx 0.4$), a New Telluride from the Good Hope Mine, Vulcan, Colorado (U.S.A.)

Marta Morana ¹ and Luca Bindi ^{2,*}

¹ Dipartimento di Scienze della Terra e dell'Ambiente, Università di Pavia, Via A. Ferrata 7, I-27100 Pavia, Italy; marta.morana01@universitadipavia.it

² Dipartimento di Scienze della Terra, Università degli Studi di Firenze, Via G. La Pira 4, I-50121 Firenze, Italy

* Correspondence: luca.bindi@unifi.it; Tel.: +39-055-275-7532

Received: 7 March 2019; Accepted: 22 March 2019; Published: 24 March 2019

Abstract: Here we describe a new mineral in the Cu-Ag-Te system, spiridonovite. The specimen was discovered in a fragment from the cameronite [ideally, $\text{Cu}_{5-x}(\text{Cu},\text{Ag})_{3+x}\text{Te}_{10}$] holotype material from the Good Hope mine, Vulcan, Colorado (U.S.A.). It occurs as black grains of subhedral to anhedral morphology, with a maximum size up to 65 μm , and shows black streaks. No cleavage is observed and the Vickers hardness (VHN_{100}) is 158 $\text{kg}\cdot\text{mm}^{-2}$. Reflectance percentages in air for R_{min} and R_{max} are 38.1, 38.9 (471.1 nm), 36.5, 37.3 (548.3 nm), 35.8, 36.5 (586.6 nm), 34.7, 35.4 (652.3 nm). Spiridonovite has formula $(\text{Cu}_{1.24}\text{Ag}_{0.75})_{\Sigma 1.99}\text{Te}_{1.01}$, ideally $(\text{Cu}_{1-x}\text{Ag}_x)_2\text{Te}$ ($x \approx 0.4$). The mineral is trigonal and belongs to the space group $P\text{-}3c1$, with the following unit-cell parameters: $a = 4.630(2)$ Å, $c = 22.551(9)$ Å, $V = 418.7(4)$ Å³, and $Z = 6$. The crystal structure has been solved and refined to $R1 = 0.0256$. It can be described as a rhombohedrally-compressed antiferroite structure, with a rough *ccp* arrangement of Te atoms. It consists of two Te sites and three *M* (metal) sites, occupied by Cu and Ag, and is characterized by the presence of edge-sharing tetrahedra, where the four-fold coordinated *M* atoms lie. The mineral and its name have been approved by the Commission of New Minerals, Nomenclature and Classification of the International Mineralogical Association (No. 2018-136).

Keywords: spiridonovite; Ag-telluride; Cu-telluride; copper; silver; Good Hoop mine; Colorado

1. Introduction

Spiridonovite is a new member of the Cu-Ag-Te system, together with rickardite [1], $(\text{Cu}_{3-x}\text{Te}_2)$, vulcanite (CuTe) [2], weissite $(\text{Cu}_{2-x}\text{Te})$ [3], cameronite $[\text{Cu}_{5-x}(\text{Cu},\text{Ag})_{3+x}\text{Te}_{10}]$ [4], and henryite $[(\text{Cu},\text{Ag})_{3+x}\text{Te}_2]$ [5]. The new mineral species was discovered in a fragment from the cameronite holotype material, sample R-934, from the Good Hope mine (38° 20' 35" N, 107° 0' 26" W), Vulcan, Colorado (U.S.A.) obtained in 1974 by the late William W. Pinch on exchange from the Smithsonian Institution, Washington D.C. (U.S.A.) [4].

The Good Hope mine was active from 1898 to 1904, and intermittently through 1930. The mineralization is hosted in mafic intrusive rock, schist and felsic volcanic rock [6]. Precious metals and tellurides are localized in quartz veins and successive supergene alteration of tellurides (altaite, galena, and goldfieldite) formed native Te and Cu-tellurides (e.g., rickardite, vulcanite, weissite), like spiridonovite.

The new mineral has been named after Ernst M. Spiridonov (b. 1938), Professor at the Department of Mineralogy, Moscow State University, Russia. He studied gold deposits of the Urals, Transbaikalia, Kamchatka, Uzbekistan, Armenia, and Bulgaria in the last fifty years and discovered 20 new mineral species, most of them ore minerals. The new mineral and mineral name have been approved by the Commission on New Minerals, Nomenclature and Classification of the International Mineralogical Association (No. 2018-136). The holotype material is deposited in the

collections of the Museo di Storia Naturale, Università degli Studi di Firenze, Via La Pira 4, I-50121, Firenze, Italy, catalogue number 3295/I.

2. Description and Physical Properties

Spiridonovite occurs as very rare crystals closely associated to rickardite, vulcanite, cameronite and native tellurium (Figure 1); its maximum grain size is about 65 μm . The mineral shows a subhedral to anhedral grain morphology without inclusions or intergrowths with other minerals.

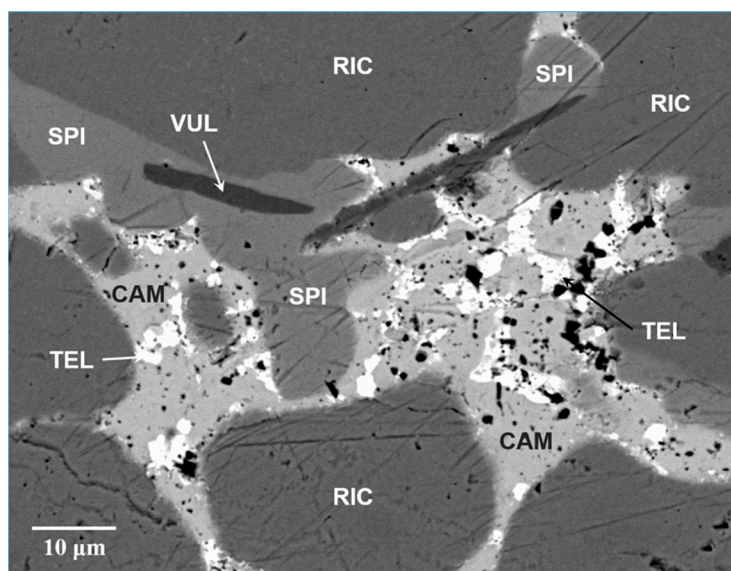


Figure 1. Scanning Electron Microscopy-BackScattered Electron (SEM-BSE) image of spiridonovite (SPI) associated with cameronite (CAM), rickardite (RIC), vulcanite (VUL) and tellurium (TEL).

Spiridonovite crystals are black, show metallic luster and black streak, and are not fluorescent. Mohs hardness, estimated from the Vickers measurements, is ~ 3 . Micro-indentation measurements, carried out with a CORE micro-indentation system, give a mean value of 158 $\text{kg}\cdot\text{mm}^{-2}$ (range 145–170). Tenacity is brittle, and cleavage is not observed. Parting is not observed, and fractures are irregular. The density could not be determined due to the small grain size. The calculated density is $4.6 \text{ g}\cdot\text{cm}^{-3}$, using the empirical formula and X-ray single-crystal data (see below).

In plane-polarize incident light, the mineral is dark bluish black, with moderate bireflectance (slightly higher than cameronite) and very weak pleochroism from light grey to a slightly greenish grey. Under crossed polars, spiridonovite shows very weak anisotropism with greyish to light-blue rotation tint. Internal reflections are absent, and there is no optical evidence of growth zonation. Reflectance values were measured in air using a MPM-200 Zeiss microphotometer equipped with a MSP-20 system processor on a Zeiss Axioplan ore microscope (Zeiss, Jena, Germany). The filament temperature was approximately 3350 K. An interference filter was adjusted, in turn, to select four wavelengths for measurement (471.1, 548.3, 586.6, and 652.3 nm). Readings were taken for specimen and standard (SiC) maintained under the same focus conditions. The diameter of the circular measuring area was 0.05 mm. Reflectance values are reported in Table 1.

Table 1. Reflectance values for spiridonovite.

R_{max}	R_{min}	λ (nm)
38.9	38.1	471.1
37.3	36.5	548.3
36.5	35.8	586.6
35.4	34.7	652.3

3. Chemical Data

A preliminary chemical analysis using EDS performed on the crystal fragment used for the structural study did not indicate the presence of elements ($Z > 9$) other than Cu, Ag and Te. However, given the minor elements found in cameronite [4], we analyzed also Bi, Pb, Zn, Fe, Sb, As, S, Se at the electron microprobe. Analyses ($n = 5$) were carried out using a JEOL 8200 microprobe (WDS mode, 25 kV, 20 nA, 1 μm beam size, counting times 20 s for peak and 10 s for background. JEOL, Tokyo, Japan). For the WDS analyses the following lines were used: $SK\alpha$, $FeK\alpha$, $CuK\alpha$, $ZnK\alpha$, $AsL\alpha$, $SeL\alpha$, $AgL\alpha$, $SbL\beta$, $TeL\alpha$, $PbM\alpha$, $BiM\beta$. The crystal fragment was found to be homogeneous within analytical error. Analytical data are given in Table 2.

Table 2. Analytical data in wt.% for spiridonovite.

Constituent	Mean	Range	Stand. dev. (σ)	Standard
Ag	27.83	25.88–28.09	0.19	Ag metal
Cu	27.12	26.02–27.94	0.16	Cu metal
Bi	0.01	0.00–0.03	0.03	synthetic Bi_2S_3
Pb	0.02	0.00–0.03	0.02	galena
Zn	0.01	0.00–0.02	0.02	synthetic ZnS
Fe	0.02	0.00–0.04	0.04	pyrite
Sb	0.01	0.00–0.02	0.02	synthetic Sb_2Te_3
As	0.02	0.00–0.03	0.03	synthetic As_2S_3
S	0.01	0.00–0.02	0.02	pyrite
Se	0.02	0.00–0.04	0.03	synthetic PtSe_2
Te	44.35	42.63–45.81	0.29	synthetic Sb_2Te_3
Total	99.42	99.15–100.55		

The empirical formula based on 3 atoms per formula unit is $(\text{Cu}_{1.24}\text{Ag}_{0.75})_{\Sigma 1.99}\text{Te}_{1.01}$, which is in excellent agreement with that derived from the structure refinement, i.e. $(\text{Cu}_{1.19}\text{Ag}_{0.81})_{\Sigma 2.00}\text{Te}$. The simplified formula is $(\text{Cu,Ag})_2\text{Te}$. The ideal formula is $(\text{Cu}_{1-x}\text{Ag}_x)_2\text{Te}$ ($x \approx 0.4$). $(\text{Cu}_{0.6}\text{Ag}_{0.4})_2\text{Te}$ requires Cu 26.28, Ag 29.74, Te 43.98, Total 100. Silver is an essential constituent in spiridonovite with the intrinsic role to stabilize the crystal structure.

4. X-ray Crystallography

X-ray powder diffraction data (Table 3) were collected on a fragment handpicked from the polished section with an Oxford Diffraction Excalibur PX Ultra diffractometer fitted with a 165 mm diagonal Onyx CCD detector and using copper radiation ($\text{CuK}\alpha$, $\lambda = 1.54138 \text{ \AA}$).

Table 3. Analytical data in wt.% for spiridonovite. 1 = observed diffraction pattern; 2 = calculated diffraction pattern obtained with the atom coordinates and occupancies reported in Table 5 (only reflections with $I_{\text{rel}} \geq 4$ are listed).

			1		2	
h	k	l	d_{obs}	I_{est}	d_{calc}	I_{calc}
0	1	2	3.78	60	3.778	67
0	0	6	3.76	20	3.759	23
1	0	4	-	-	3.268	8
1	1	0	2.317	100	2.3150	100
0	1	8	2.305	85	2.3060	99
2	0	2	-	-	1.9739	10
1	1	6	1.973	15	1.9711	21
1	0	10	-	-	1.9656	9
2	0	8	1.635	30	1.6338	30
1	2	2	-	-	1.5020	8
0	1	14	-	-	1.4947	4
3	0	0	1.338	10	1.3366	14
1	2	8	1.333	25	1.3348	27

1	0	16	1.328	10	1.3297	13
2	2	0	-	-	1.1575	8
0	2	16	-	-	1.1530	8
3	1	8	1.033	5	1.0345	11
2	1	16	-	-	1.0321	11
0	4	8	-	-	0.9445	5
1	3	16	-	-	0.8730	9
1	1	24	-	-	0.8706	10

Single-crystal X-ray studies were carried out using an Oxford Diffraction Xcalibur diffractometer equipped with an Oxford Diffraction CCD detector, with graphite-monochromatized MoK α radiation ($\lambda = 0.71073 \text{ \AA}$). Crystal data and details of the intensity data collection and refinement are reported in Table 4.

Table 4. Crystal and experimental data for spiridonovite.

Crystal size (mm)	0.040 \times 0.050 \times 0.060
Cell setting	Trigonal
Space group	<i>P</i> -3 <i>c</i> 1 (#165)
<i>a</i> , <i>c</i> (\AA)	4.630(2), 22.550(10)
<i>V</i> (\AA^3)	418.7(4)
<i>Z</i>	6
Temperature (K)	293(2)
$2\theta_{\text{max}}$ ($^\circ$)	64.30
Measured reflections	2155
Unique reflections	435
Reflections with $F_o > 4\sigma(F_o)$	103
R_{int}	0.0312
$R\sigma$	0.0270
Range of <i>h</i> , <i>k</i> , <i>l</i>	−5−5; −6−6; −32−32
$R1 [F_o > 4\sigma(F_o)]$	0.0256
$R1$ (all data)	0.0304
w <i>R</i> (on F^2)	0.0696
GooF	0.991
No. least-squares parameters	18
Max. and min. resid. peak ($e \text{ \AA}^{-3}$)	0.38; −0.24

Single-crystal X-ray diffraction intensity data were integrated and corrected for standard Lorentz polarization factors with the *CrysAlis^{pro}* package (Oxford Diffraction, Oxford, UK [7]). The program ABSPACK in *CrysAlis* RED [8] was used for the absorption correction. A total of 435 unique reflections were collected. Systematic absences were consistent with the space groups *P*-3*c*1 and *P*3*c*1. The statistical tests on the distribution of $|E|$ values ($|E^2-1| = 0.977$) indicated the presence of an inversion center and so the *P*-3*c*1 space group was chosen. The structure was solved and refined using the program *Shelx-97* [9]. The site occupation factor (s.o.f.) at the cation sites was allowed to vary (Cu vs. Ag for the *M* positions and Te vs. structural vacancy for the anionic positions) using scattering curves for neutral atoms taken from the *International Tables for X-ray Crystallography* [10]. The Te sites were found fully occupied by tellurium and then fixed in the subsequent refinement cycles. Final atomic coordinates and equivalent isotropic displacement parameters are given in Table 5, whereas selected bond distances are shown in Table 6.

Table 5. Atoms, site-occupancy factors (s.o.f.), Wyckoff positions, atom coordinates and isotropic displacement parameters (\AA^2) for spiridonovite.

Atom	s.o.f	Wyckoff	x/a	y/b	z/c	U_{eq}
M1	$\text{Cu}_{0.60(1)}\text{Ag}_{0.40}$	4c	0	0	0.37419(7)	0.0623(5)
M2	$\text{Cu}_{0.64(1)}\text{Ag}_{0.36}$	4d	$\frac{1}{3}$	$\frac{2}{3}$	0.79165(7)	0.0628(4)
M3	$\text{Cu}_{0.55(1)}\text{Ag}_{0.45}$	4d	$\frac{1}{3}$	$\frac{2}{3}$	0.04146(7)	0.0634(4)
Te1	$\text{Te}_{1.00}$	2b	0	0	0	0.0646(5)
Te2	$\text{Te}_{1.00}$	4d	$\frac{1}{3}$	$\frac{2}{3}$	0.66635(3)	0.0699(5)

Table 6. Selected bond distances (\AA) for spiridonovite.

M1-	Te1	2.837(2)	M2-	Te2	2.826(2)	M3-	Te2	2.816(2)
	Te2	2.825(1) ($\times 3$)		Te2	2.836(1) ($\times 3$)		Te1	2.832(1) ($\times 3$)

4. Results and Discussion

From a chemical point of view, spiridonovite is close to weissite (Cu_{2-x}Te). However, while weissite can be Ag-free, the presence of Ag in spiridonovite enlarges the coordination polyhedra, creating a different topology with respect to that of weissite, and stabilizing the structure. Indeed, spiridonovite can be seen as a rhombohedrally-compressed antiferroite structure, with a rough *ccp* arrangement of Te atoms, which exhibit a cubic arrangement. On the contrary, Te atoms exhibit a highly distorted *hcp* arrangement in weissite, thus producing short Cu-Cu distances and partially occupied Cu sites. Weissite has a complex structure with 24 independent Cu and 12 Te atoms showing significantly different crystal-chemical environments [3], while the crystal structure of spiridonovite is far simpler and comprises two Te sites and three M sites, which are occupied by Cu and minor Ag, as reported in Table 5.

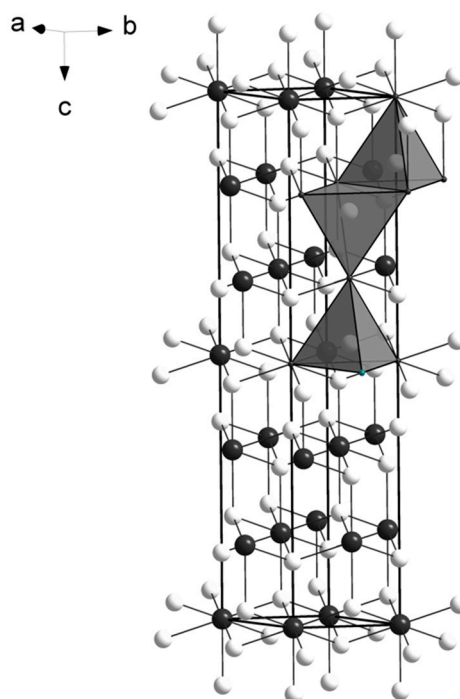


Figure 2. The crystal structure of spiridonovite. M (Cu,Ag) sites and Te atoms are given as white and black circles, respectively. The tetrahedral coordination of the M sites is shown as isolated polyhedra. The unit cell and the orientation of the structure are outlined.

The *M* atoms have four-fold coordination, creating an arrangement of edge-sharing tetrahedra on (110), similarly to what reported for the crystal structure of empressite (AgTe), that shows sheets of edge-sharing AgTe₄ tetrahedra [11]. The main difference between the two structures is the environment of tellurium atoms: in empressite there are Te₃ groups, a rare feature in mineral crystal structures, so far reported only in empressite and krennerite [12]. The spiridonovite structure is shown in Figure 2. The presence of Ag affects the bond distances (in the range 2.82–2.84 Å; Table 6) that are larger than those reported for Cu tellurides, such as vulcanite (CuTe) [13], rickardite (Cu_{3-x}Te₂) [14], cameronite (Cu_{5-x}(Cu,Ag)_{3+x}Te₁₀ [4]), weissite (Cu_{2-x}Te) [3], and henryite ((Cu,Ag)_{3+x}Te₂) [5]. Conversely, they are smaller than those observed in Ag-tellurides, such as empressite (AgTe) [11] and hessite (Ag₂Te) [15]. No short metal-metal contacts are observed. Bond valence sums (Table 7), calculated according to the parameters given by Brese and O’Keeffe [16], and taking into account the refined occupancies (Table 5), confirm the validity of the structural model.

Table 7. Bond valence sums (v.u.) for spiridonovite

Atom	M1	M2	M3	ΣTe
Te1	0.265 ^{x2→}		0.277 ^{x3↓x6→}	2.192
Te2	0.274 ^{x3↓x3→}	0.267 0.260 ^{x3↓x4→}	0.286	2.148
	1.087	1.047	1.117	

All the minerals belonging to the Cu-Ag-Te system are shown in Table 8, together with some crystallographic detail.

If we consider a tripled *a* parameter for spiridonovite, we get the cell: *a* = 13.89 and *c* = 22.55 Å. Such a metric has some analogy with that of the β^{III} synthetic compound of the Cu-Te system [17], which exhibits a hexagonal symmetry and *a* = 12.54 and *c* = 21.71 Å. The cell enlargement observed for spiridonovite could be due to the presence of Ag replacing Cu.

Table 8. Minerals belonging to the Cu-Ag-Te system.

Mineral [ref]	Formula	Space Group	Cell Values (Å)	V(Å ³)	Z
cameronite [4]	Cu _{5-x} (Cu,Ag) _{3+x} Te ₁₀ (<i>x</i> = 0.43)	C2/c	<i>a</i> = 17.906(1) <i>b</i> = 17.927(1) <i>c</i> = 21.230(2) β = 98.081(8)°	6747.2(8)	14
empressite [11]	AgTe	<i>Pmnb</i>	<i>a</i> = 8.882(1) <i>b</i> = 20.100(5) <i>c</i> = 4.614(1)	823.7(3)	16
henryite [5]	(Cu,Ag) _{3+x} Te ₂ (<i>x</i> = 0.40)	<i>Fd-3c</i>	<i>a</i> = 12.1987(5)	1815.3(2)	16
hessite [15]	Ag ₂ Te	<i>P2₁/c</i>	<i>a</i> = 8.164(1) <i>b</i> = 4.468(1) <i>c</i> = 8.977(1) β = 124.16(1)°	271.0(1)	4
krennerite [12]	(Au _{1-x} Ag _x)Te ₂ (<i>x</i> = 0.2)	<i>Pma2</i>	<i>a</i> = 16.58(3) <i>b</i> = 8.849(3) <i>c</i> = 4.464(3)	654(1)	8
rickardite [14]	Cu _{3-x} Te ₂	<i>Pmmm</i>	<i>a</i> = 3.9727(4) <i>b</i> = 4.0020(5) <i>c</i> = 6.1066(3)	97.1(1)	2

vulcanite [13]	CuTe	<i>Pmnn</i>	$a = 3.155(1)$ $b = 4.092(1)$ $c = 6.956(1)$	89.80(3)	2
weissite [3]	Cu_{2-x}Te ($x = 0.21$)	<i>P3m1</i>	$a = 8.3124(7)$ $c = 21.546(1)$	1289.3(2)	24

However, as demonstrated by [18], the β^{III} synthetic phase is actually an intermetallic compound, with short Cu-Cu and Te-Te contacts, and thus different from spiridonovite. Cameronite ($\text{Cu}_{5-x}(\text{Cu},\text{Ag})_{3+x}\text{Te}_{10}$ [4]) and weissite (Cu_{2-x}Te) [3] have a similar intermetallic nature, showing short bond distances between the metals, characterized by the presence of typical “interpenetrated tetrahedra” due to the short Cu-Cu, Te-Te, and Cu-Te distances.

Supplementary Materials: The following are available online at www.mdpi.com/link, CIF: spiridonovite.

Author Contributions: Luca Bindi found the new mineral and carried out the electron microprobe analyses and the X-ray single-crystal experiments; Luca Bindi and Marta Morana analyzed the data; Marta Morana wrote the paper with input from Luca Bindi.

Funding: The research was funded by MIUR, project “TEOREM deciphering geological processes using Terrestrial and Extraterrestrial ORE Minerals”, prot. 2017AK8C32 (PI: Luca Bindi), and by “progetto d’Ateneo 2016, University of Firenze” to Luca Bindi.

Conflicts of Interest: The authors declare no conflict of interest.

References

1. Ford, W.E. Rickardite, a New Mineral. *Am. J. Sci.* **1903**, *15*, 69.
2. Cameron, E.N.; Threadgold, I.M. Vulcanite, a new copper telluride from Colorado, with notes on certain associated minerals. *Am. Mineral.* **1961**, *46*, 258–268.
3. Bindi, L.; Carbone, C.; Belmonte, D.; Cabella, R.; Bracco, R. Weissite from Gambatesa mine, Val Graveglia, Liguria, Italy: occurrence, composition and determination of the crystal structure. *Mineral. Mag.* **2013**, *77*, 475–483.
4. Bindi, L.; Pinch, W.W. Cameronite, $\text{Cu}_{5-x}(\text{Cu},\text{Ag})_{3+x}\text{Te}_{10}$ ($x=0.43$), from the Good Hope Mine, Vulcan, Colorado: crystal structure and revision of the chemical formula. *Can. Mineral.* **2014**, *52*, 423–432.
5. Bindi, L. Chemical and structural characterization of henryite, $(\text{Cu},\text{Ag})_{3+x}\text{Te}_2$ ($x\approx 0.40$): A new structure type in the (Ag)–Cu–Te system. *Solid State Sci.* **2014**, *38*, 108–111.
6. Hartley, T.D. Geology and Mineralization of the Vulcan-Good Hope Massive Sulfide Deposit, Gunnison County, Colorado. In *Gunnison Gold Belt and Powderhorn Carbonatite Field Trip Guidebook: Dregs*; Handfield, R.C., Ed.; Denver Region Exploration Geologists Society: Denver, CO, USA 1983; pp. 19–27.
7. Oxford Diffraction Ltd. *CrysAlis RED*; Oxford Diffraction Ltd.: Abingdon, UK, 2006.
8. Oxford Diffraction Ltd. *ABSPACK in CrysAlis RED*; Oxford Diffraction Ltd.: Abingdon, UK, 2006.
9. Sheldrick, G.M. A short history of SHELX. *Acta Crystallogr. Sect. A* **2008**, *64*, 112–122.
10. Wilson, A.J.C. *International Tables for Crystallography: Mathematical, Physical, and Chemical Tables*; International Union of Crystallography: Chester, UK, 1992; Volume 3.
11. Bindi, L.; Spry, P.G.; Cipriani, C. Empressite, AgTe , from the Empress-Josephine mine, Colorado, U.S.A.: Composition, physical properties, and determination of the crystal structure. *Am. Mineral.* **2004**, *89*, 1043–1047.
12. Pertlik, F. Crystal Chemistry of Natural Tellurides II: Redetermination of the Crystal Structure of Krennerite, $(\text{Au}_{1-x}\text{Ag}_x)\text{Te}_2$ with $x \sim 0.2$. *Tschermaks Mineral. Petrogr. Mitt.* **1984**, *33*, 253–262.
13. Pertlik, F. Vulcanite, CuTe : hydrothermal synthesis and crystal structure refinement. *Mineral. Petrol.* **2001**, *71*, 149–154.
14. Schutte, W.J.; De Boer, J.L. Determination of the incommensurately modulated structure of $\text{Cu}_{3-x}\text{Te}_2$. *Acta Crystallogr. Sect. B* **1993**, *49*, 398–403.
15. van der Lee, A.; de Boer, J.L. Redetermination of the structure of hessite, Ag_2Te -III. *Acta Crystallogr. Sect. C* **1993**, *49*, 1444–1446.

16. Brese, N.E.; O’Keeffe, M. Bond-valence parameters for solids. *Acta Crystallogr. Sect. B* **1991**, *4*, 192–197.
17. Baranova, R.V.; Avilov, A.S.; Pinsker, Z.G. Determination of the crystal structure of the hexagonal phase beta III in the Cu-Te system by electron diffraction. *Sov. Phys. Crystallogr.* **1974**, *18*, 736–740.
18. Pashinkin, A.S.; Fedorov, V.A. Phase Equilibria in the Cu-Te System. *Inorg. Mater.* **2003**, *39*, 539–554.



© 2019 by the authors. Submitted for possible open access publication under the terms and conditions of the Creative Commons Attribution (CC BY) license (<http://creativecommons.org/licenses/by/4.0/>).